

# Class Incremental Online Streaming Learning

Soumya Banerjee<sup>1</sup>, Vinay Kumar Verma<sup>2</sup>, Toufiq Parag<sup>3</sup>, Maneesh Singh<sup>3</sup>, Vinay P. Namboodiri<sup>1,4</sup>  
<sup>1</sup>IIT Kanpur, India <sup>2</sup>Duke University, USA <sup>3</sup>Verisk Analytics, NJ, USA <sup>4</sup>University of Bath, UK

soumyab@cse.iitk.ac.in, vinaykumar.verma@duke.edu, toufiq.parag@verisk.com  
maneesh.singh@verisk.com, vpn22@bath.ac.uk

## Abstract

A wide variety of methods have been developed to enable lifelong learning in conventional deep neural networks. However, to succeed, these methods require a ‘batch’ of samples to be available and visited multiple times during training. While this works well in a static setting, these methods continue to suffer in a more realistic situation where data arrives in online streaming manner. We empirically demonstrate that the performance of current approaches degrades if the input is obtained as a stream of data with the following restrictions: (i) each instance comes one at a time and can be seen only once, and (ii) the input data violates the i.i.d assumption, i.e., there can be a class-based correlation. We propose a novel approach (CIOSL) for the class-incremental learning in an online streaming setting to address these challenges. The proposed approach leverages implicit and explicit dual weight regularization and experience replay. The implicit regularization is leveraged via the knowledge distillation, while the explicit regularization incorporates a novel approach for parameter regularization by learning the joint distribution of the buffer replay and the current sample. Also, we propose an efficient online memory replay and replacement buffer strategy that significantly boosts the model’s performance. Extensive experiments and ablation on challenging datasets show the efficacy of the proposed method.

## 1. Introduction

In this paper, we aim to achieve true continual learning by solving an extreme and restrictive form of lifelong learning. Predominantly, the more popular and successful methods in continual learning operate in *incremental batch learning* (IBL) scenarios [1, 23, 37, 40, 42]. In IBL, we assume that current task data is available in batches during training, and the learner visits them sequentially multiple times. However, these methods are ill-suited in a continuously changing environment, where the learner needs to quickly adapt to the newly available data without catastrophic forgetting [12] in

an *online manner*.

The ability to continually learn effectively from streaming data with no catastrophic forgetting is a challenge that has not received widespread attention [14]. However, its utility is apparent, as it enables the practical deployment of autonomous AI agents. In the real world, an autonomous agent continuously encounters new examples of a novel or previously observed classes. To adapt to these new examples, it is often required to train the AI agent with these new instances immediately without disrupting its service. It is infeasible to wait and aggregate a ‘batch’ of new samples for learning on the new data. Moreover, the ability to learn online in a *streaming setting* is not only practical, but a step towards enabling true lifelong learning on embodied AI agents in a dynamic, non-stationary environment.

In this work, we are interested in learning continuously in *online streaming setting*, where a learner needs to learn from a single sample at a time, with no catastrophic forgetting, in a *single-pass*. The model can visit any part of data only once, and it can be evaluated any time without waiting for termination of training. In addition, we also aim to evaluate the model in *class-incremental setting*, such that at test time, we consider the label space over all the observed classes so far. This is in contrast to task-incremental learning methods such as VCL [31], which requires task labels to be specified during inference. While some recent works aim at *online learning* and consider *class-incremental learning* setting, these methods are not suitable in the *streaming learning* setting. For instance, GDumb [33] suggests that storing data points with a greedy-sampler and retraining before inference outperforms existing approaches. However, one does visit data points multiple times during retraining, which violates the *single-pass* learning constraint. AGEM [7], another online learning approach, is based on projected-gradient-descent, also suffers severe forgetting in *streaming setting*. Finally, the recently proposed *streaming learning* approach, REMIND [15] is limited in terms of requiring a significant amount of cached data. Our work addresses all these limitations in a principled manner with a limited amount of information. Figure 1 compares the proposed method with



Figure 1.  $\Omega_{\text{all}}$  results for ‘batch’, ‘online’ and ‘streaming’ versions of baselines on iCubWorld 1.0 on (i) Class-iid, and (ii) Class-instance ordering. An empty plot in A-GEM indicates, we were unable to conduct experiment due to compatibility issues.

the recent strong baselines. We observe that *Our-model* outperforms the baselines by a significant margin in *all three different lifelong learning* settings. It implies that a learning method in the most restrictive setting can be thought of as a universal method for all lifelong learning settings with the widest possible applicability.

We propose a novel method, ‘*Class Incremental Online Streaming Learning*’ (CIOSL), which enables lifelong learning in *online streaming setting* by leveraging tiny episodic memory replay and regularization. It regularises the model from two sources. One focuses on regularizing the model parameters explicitly in an online Bayesian framework, while the other regularises implicitly by enforcing the updated model to produce similar outputs for previous models on the past observed data. Our approach is jointly trained with buffer replay and current task samples by incorporating the likelihood of the replay and current samples. As a result, we do not need explicit finetuning with buffer samples. We propose a novel online loss-aware strategy for buffer replacement and coreset sample selection that significantly boosts the model’s performance. Our approach only requires a small subset of samples for memory replay, and we do not use full buffer replay like past approaches [14]. Our experimental results on four benchmark datasets demonstrate the effectiveness as well as superiority of the proposed method to circumvent catastrophic forgetting over state-of-the-art baselines, and the extensive ablations validate the components of our method.

Our contributions can be summarised as follows: (i) we propose a novel dual regularization framework (CIOSL), comprising an online Bayesian framework as well as a functional regularizer, to overcome catastrophic forgetting in challenging *online streaming learning* scenario, (ii) we propose a novel online loss-aware buffer replacement and sampling strategy which significantly boosts the model’s performance, (iii) we empirically show that selecting a subset of samples from memory and computing the joint likelihood with the current sample is highly efficient, and enough to avoid explicit finetuning, and (iv) we experimentally show that our method significantly outperforms the state-of-the-art baselines.

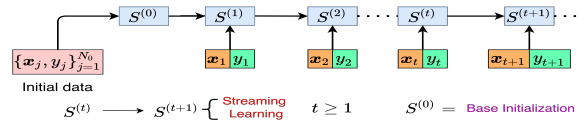


Figure 2. **Proposed streaming learning framework.**  $S^{(t)}$  represents the evolving state of the model after learning the  $t$ -th example, i.e.,  $\mathcal{D}_t = \{\mathbf{d}_t\} = \{(\mathbf{x}_t, \mathbf{y}_t)\}$ .

## 2. Problem Formulation

*Online streaming learning* (OSL) or *streaming learning* is the extreme case of online learning, where the data arrives sequentially one at a time, and the model needs to learn in a ‘*single-pass*’. Let us consider that we have a dataset  $\mathcal{D}$  with  $T$  task sequences, i.e.  $\mathcal{D} = \{\mathcal{D}_t\}_{t=1}^T$ , where  $\mathcal{D}_t = \{(\mathbf{x}_j, \mathbf{y}_j)\}_{j=1}^{N_t}$ . In *streaming learning*, it is assumed that  $N_t = 1$  for all  $t$ , unlike *incremental batch learning* (IBL) and *online learning* approaches, where it is assumed  $N_t \gg 1$  for all  $t$ . In addition, the model cannot loop over any part of the dataset, i.e., *single-pass* learning, and it can be evaluated immediately rather waiting for termination of training. This is in contrast to the *incremental batch learning* [1, 23] and *online learning* [33] approaches which allow visiting data-batches  $\mathcal{D}_t$  sequentially for multiple times and fine-tuning the network parameters with the buffer samples before inference, respectively. Furthermore, the data coming in *streaming setting* can be temporally contiguous, i.e., there could be a class based correlation, and the memory usage must be minimal. Finally, the model is evaluated in *class incremental setting*, such that, at test time, the label space is considered over all the classes observed so far.

## 3. Online Streaming Learning Framework

In this section, we introduce a ‘*class incremental online-streaming learning*’ framework (CIOSL) which trains a convolutional neural network (CNN) in *streaming setting*, as depicted in Figure 2. Formally, a limited number of samples are used to train the model offline during base initialization,  $S^{(0)}$ . Then in each incremental step,  $\forall t > 0$ ,  $S^{(t)}$ , it observes a new example  $(\mathbf{x}_t, \mathbf{y}_t)$ , and the parameters are updated with a single step posterior computation. To avoid catastrophic forgetting, we use dual regularization by proposing implicit

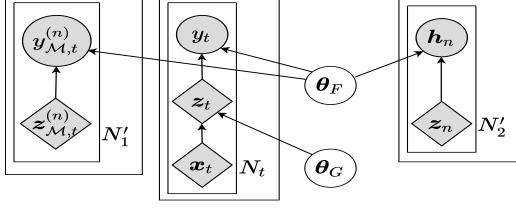


Figure 3. Graphical model of the proposed neural network training in ‘streaming-setting’, as discussed in Section 3.1.

and explicit regularization over the model parameters. Section 3.1 discusses the detailed regularization model. We also propose a novel online samples selection strategy for replay and buffer replacement which significantly improves model performance. We use a tiny episodic memory, and select only few informative past samples for replay *instead of replaying the whole buffer*, Section 3.2 and 3.3 are dedicated to the detailed discussion about the buffer policy.

Formally, we separate the CNN into two neural networks: (i) *non-plastic* feature extractor  $G(\cdot)$  consisting the first few layers of the CNN, and (ii) *plastic* neural network  $F(\cdot)$  consisting the final layers of the CNN. For a given input image  $\mathbf{x}$ , the predicted class label is computed as:  $y = F(G(\mathbf{x}))$ . We initialize the parameters of the feature extractor  $G(\cdot)$  and keep it frozen throughout online streaming setting. We use a *Bayesian-neural-network* (BNN) [30] as the *plastic* network  $F(\cdot)$ , and optimize its parameters with sequentially coming data in *streaming setting*.

### 3.1. Learning in Online Streaming Scenario

Online updating naturally emerges from the Bayes’ rule; given the posterior  $p(\theta|\mathcal{D}_{1:t-1})$ , whenever a new data  $\mathcal{D}_t = \{\mathbf{d}_t\} = \{\mathbf{x}_t, y_t\}$  comes in, we can compute a new posterior  $p(\theta|\mathcal{D}_{1:t})$  by combining the previous posterior and the new data-likelihood, i.e.,  $p(\theta|\mathcal{D}_{1:t}) \propto p(\mathcal{D}_t|\theta) p(\theta|\mathcal{D}_{1:t-1})$ , where the old posterior is treated as the prior. However, for any complex model, exact Bayesian inference is not tractable, and an approximation is needed. A Bayesian neural network commonly approximates the posterior with a variational posterior  $q(\theta)$  by maximizing the evidence-lower-bound (ELBO) [3]. However, optimizing the ELBO to approximate the posterior  $p(\theta|\mathcal{D}_{1:t})$  only with data  $\mathcal{D}_t$  can fail in streaming setting [13]. Furthermore, we evaluate the model’s performance in *class incremental setting*, such that, at test time the label space is considered over all the classes have been observed till the time instance  $t$ . Moreover, training only with  $\mathcal{D}_t$  makes the model biased towards the new data or task and parameter regularization is not sufficient to overcome forgetting. To overcome these limitations, we include a ‘fixed-sized’ tiny episodic memory for storing a small representative subset ( $\leq 5\%$ ) of all the observed samples. Instead of storing the raw input  $\mathbf{x}$ , we store the embedding

$\mathbf{z} = G(\mathbf{x})$ , where  $\mathbf{z} \in \mathbb{R}^d$ . Storing the embeddings save a significant amount of memory, and also saves the model from doing a forward pass through the convolutional layers, making the training procedure computationally highly efficient.

During training, we select a subset of samples from memory *instead of replaying the whole buffer*, and replay them with the new data  $\mathcal{D}_t = \{\mathbf{d}_t\} = \{\mathbf{x}_t, y_t\}$ . Therefore, the new posterior computation can be written as follows:  $p(\theta|\mathcal{D}_{1:t}) \propto p(\mathcal{D}_t|\theta)p(\mathcal{D}_{\mathcal{M},t}|\theta)p(\theta|\mathcal{D}_{1:t-1})$ , which we approximate with a variational posterior  $q_t(\theta)$  as follows:

$$\mathcal{L}_t^1(\theta) = \arg \min_{q \in \mathcal{Q}} \text{KL} \left( q_t(\theta) \parallel \frac{1}{Z_t} q_{t-1}(\theta) p(\mathcal{D}_t|\theta) p(\mathcal{D}_{\mathcal{M},t}|\theta) \right) \quad (1)$$

where  $\mathcal{D}_{\mathcal{M},t} \subset \mathcal{M}$  represents the subset of samples selected from the memory  $\mathcal{M}$  for replaying at time  $t$ , and  $\mathcal{D}_t$  represents the new data arriving at time  $t$ . Note that Eq. (1) is significantly different from VCL [31], where they assume *multi-task/task-incremental learning setting* with separate *head networks*, and incorporates the coreset samples only during explicit finetuning before inference.

The above minimization is equivalent to maximization of the evidence-lower-bound (ELBO):

$$\begin{aligned} \mathcal{L}_t^1(\theta) = & \mathbb{E}_{\theta \sim q_t(\theta)} [\log p(y_t|\theta, G(\mathbf{x}_t))] \quad (2) \\ & + \sum_{n=1}^{N'_1} \mathbb{E}_{\theta \sim q_t(\theta)} \left[ \log p(y_{\mathcal{M},t}^{(n)}|\theta, \mathbf{z}_{\mathcal{M},t}^{(n)}) \right] \\ & - \lambda_1 \cdot \text{KL} (q_t(\theta) \parallel q_{t-1}(\theta)) \end{aligned}$$

where  $\mathcal{D}_t = \{\mathbf{d}_t\} = \{\mathbf{x}_t, y_t\}$ ,  $\mathcal{D}_{\mathcal{M},t} = \{\mathbf{d}_{\mathcal{M},t}^{(n)}\}_{n=1}^{N'_1} = \{(\mathbf{z}_{\mathcal{M},t}^{(n)}, y_{\mathcal{M},t}^{(n)})\}_{n=1}^{N'_1}$ ,  $|\mathcal{D}_{\mathcal{M},t}| = N'_1 \ll |\mathcal{M}|$ ,  $\mathcal{D}_{\mathcal{M},t} \subset \mathcal{M}$ , and  $\lambda_1$  is a hyper-parameter.

While the KL-divergence minimization (in Eq. (2)) between prior and the posterior ensures minimal changes in the network parameters, initialization of the prior with the posterior at each time can introduce information loss in the network for a longer sequence of streaming data. We overcome such limitation with a functional/implicit regularizer, which encourages the network to mimic the output responses as produced in the past for the observed samples. Specifically, we minimize the KL-divergence between the class-probability scores obtained in past and current time  $t$ :

$$\sum_{n=1}^{t-1} \mathbb{E}_{\theta \sim q_t(\theta)} [\text{KL}(\text{softmax}(\mathbf{h}_n) \parallel F_{\theta}(G(\mathbf{x}_n)))] \quad (3)$$

where  $\mathbf{x}_n$  and  $\mathbf{h}_n$  represents input examples and the logits obtained while training on  $\mathcal{D}_n$  respectively.

However, the objective in Eq. (3) requires the availability of the embeddings and the corresponding logits for all the past observed data. Since storing all the past data is not feasible, we only store the logits for all samples in memory

$\mathcal{M}$ . During training, we uniformly select  $N'_2$  samples along with their logits and optimize the following objective:

$$\mathcal{L}_i^2(\theta) = \sum_{n=1}^{N'_2} \mathbb{E}_{\theta \sim q_t(\theta)} [\text{KL}(\text{softmax}(\mathbf{h}_n) \parallel F_\theta(\mathbf{z}_n))] \quad (4)$$

where (i)  $\mathbf{z}_n$  and  $\mathbf{h}_n$  represents feature-map and corresponding logits, and (ii)  $N'_2 \ll |\mathcal{M}|$ .

Under the mild assumptions of knowledge distillation [16], the optimization in Eq. (4) is equivalent to minimization of the Euclidean distance between the logits, and the optimization objective can be written as:

$$\mathcal{L}_i^2(\theta) = \lambda_2 \cdot \sum_{n=1}^{N'_2} \mathbb{E}_{\theta \sim q_t(\theta)} [\|\mathbf{h}_n - f_\theta(\mathbf{z}_n)\|_2^2] \quad (5)$$

where (i)  $f(\cdot)$  represents the plastic network  $F(\cdot)$  without the softmax activation, and (ii)  $\lambda_2$  is a hyper-parameter.

Training the plastic network (BNN)  $F(\cdot)$  requires specification of  $q(\theta)$  and, in this work, we model  $\theta$  by stacking up the parameters (weights & biases) of the network  $F(\cdot)$ . We use a Gaussian mean-field posterior  $q_t(\theta)$  for the network parameters, and choose the prior distribution, i.e.,  $q_0(\theta) = p(\theta)$ , as multivariate Gaussian distribution. We train the network  $F(\cdot)$  by maximizing the ELBO in Eq. (2) and minimizing the Euclidean distance in Eq. (5). For memory replay in Eq. (2), we select samples using strategies mentioned in Section 3.2, and we use *uniform sample* selection strategy to select samples from memory to be used in Eq. (5).

### 3.2. Informative Past Sample Selection For Replay

**Uniform Sampling (Uni).** In this approach, samples are selected uniformly random from the memory.

**Uncertainty-Aware Positive-Negative Sampling (UAPN).** UAPN selects  $N'_1/2$  samples with the highest uncertainty scores (negative samples) and  $N'_1/2$  samples with the lowest uncertainty scores (positive samples). Empirically, we observe that this sample selection strategy results in the best performance. We measure the predictive uncertainty [5] for an input  $\mathbf{z}$  with BNN  $F(\cdot)$  as follows:

$$\Phi(\mathbf{z}) \approx - \sum_c \left( \frac{\sum_k p(\hat{y} = c | \mathbf{z}, \theta^k)}{k} \right) \log \left( \frac{\sum_k p(\hat{y} = c | \mathbf{z}, \theta^k)}{k} \right) \quad (6)$$

where  $p(\hat{y} = c | \mathbf{z}, \theta^k)$  is the predicted softmax output for class  $c$  using the  $k$ -th sample of weights  $\theta^k$  from  $q(\theta)$ . We use  $k = 5$  samples for uncertainty estimation.

**Loss-Aware Positive-Negative Sampling (LAPN).** LAPN selects  $N'_1/2$  samples with the highest loss-values (negative-samples), and  $N'_1/2$  samples with the lowest loss-values (positive-samples). Empirically we observe that the combination of most and least certain samples shows a significant performance boost since one ensures quality while the other ensures diversity for the memory replay.

### 3.3. Memory Buffer Replacement Policy

For memory replay, we use a ‘*fixed-sized*’ tiny episodic memory. However, in a lifelong learning setting, data may come indefinitely, implying that the capacity of the replay buffer will be quickly exhausted. To combat such an issue, we employ a replay buffer replacement policy which replaces a previously stored sample with a new instance if the buffer is full. Otherwise, the new instance is stored.

**Loss-Aware Weighted Class Balancing Replacement (LAWCBBR).** In this approach, whenever a new sample comes in and the buffer is full, we remove a sample from the class with maximum number of samples present in the buffer ( $y_r = \arg \max \text{ClassCount}(\mathcal{M})$ ). However, instead of removing an example uniformly, we weigh each sample of the majority class inversely w.r.t their loss ( $w_i^{y_r} \propto \frac{1}{l_i^{y_r}}$ ) and use these weights as the replacement probability; the lesser the loss, the more likely to be removed.

**Loss-Aware Weighted Random Replacement With A Reservoir (LAWRRR).** In this approach, we propose a novel variant of reservoir sampling [41] to replace an existing sample with the new sample when the buffer is full. We weigh each stored sample inversely w.r.t the loss ( $w_i \propto \frac{1}{l_i}$ ), and proportionally to the total number of examples of that class in which the sample belongs present in the buffer ( $w_i \propto \text{ClassCount}(\mathcal{M}, y_i)$ ). Whenever a new example satisfies the replacement condition of reservoir sampling, we combine these two scores and use that as the replacement probability; the higher the weight, the more likely to be replaced.

### 3.4. Making Sampling Strategies Online

Loss-aware sampling strategies require computing the loss-values of each stored sample in each incremental step, resulting in a computationally expensive learning process. To overcome this issue, we propose the following online update policy of the loss-values: (i) for each sample stored in memory, we keep the corresponding loss-value, (ii) whenever a sample is selected for memory replay, we replace the previously computed loss-value with the new loss-value at time  $t$ ; furthermore, we update the past logits with the newly computed logits, as changes in the loss-value reflect changes in the logits, too. To accommodate the online updating of loss-values, we propose to keep the loss-value in memory for each stored sample; however, since it is just a scalar value, the storage cost is negligible. To make uncertainty-aware sampling online, we store the uncertainty scores in memory and update them in a similar manner; the storage cost remains negligible, as it is another scalar value.

### 3.5. Feature Extractor

In this work, we separate the representation learning, i.e., learning the feature extractor  $G(\cdot)$ , and the classifier learn-

ing, i.e., learning the plastic network  $F(\cdot)$ . Similar to several existing continual learning approaches [14, 15, 20, 43], we initialize the feature extractor  $G(\cdot)$  with the weights learned through supervised visual representation learning [25], and keep them fixed throughout *streaming learning*. The motivation to use a pre-trained feature extractor is that the features learned by the first few layers of the neural networks are highly transferable and not specific to any particular task or dataset and can be applied to several different task(s) or dataset(s) [45]. Moreover, it is hard to learn generalized visual features, which can be used across all the classes [46] with having access to only a single example at each time instance.

In our experiments, for all the baselines along with CIOSL, we use Mobilenet-V2 [38] pre-trained on ImageNet [36] as the base architecture for the visual feature extractor. It consists of a convolutional base and a classifier network. We remove the classifier network and use the convolutional base as the feature extractor  $G(\cdot)$  to obtain embedding that is fed to the plastic network BNN  $F(\cdot)$ . For details on the plastic network used for other baselines, refer to Section 5.3.

## 4. Related Work

Parameter-isolation-based approaches train different subsets of model parameters on sequential tasks. PNN [37], DEN [44] expand the network to accommodate the new task. PathNet [11], PackNet [29], Piggyback [28], and HAT [39] train different subsets of network parameters on each task.

Regularization-based approaches use an extra regularization term in the loss function to enable continual learning. LWF [27] uses knowledge distillation [16] loss to prevent catastrophic forgetting. EWC [23], IMM [26], and MAS [1] regularize by penalizing changes to the important weights of the network.

Rehearsal-based approaches replay a subset of past training data during sequential learning. iCaRL [34], SER [17], and TinyER [8] use memory replay when training on a new task. DER [4] uses knowledge distillation and memory replay while learning a new task. DGR [40], MeRGAN [42], and CloGAN [35] retain the past task(s) distribution with a generative model and replay the synthetic samples during incremental learning. Our approach also leverages memory replay from a tiny episodic memory; however, we store the feature-maps instead of raw inputs.

Variational Continual Learning (VCL) [31] leverages Bayesian inference to mitigate catastrophic forgetting. However, the approach, when naïvely adapted, performs poorly in the *streaming learning setting*. Additionally, it also needs task-id during inference. Furthermore, the explicit finetuning with the buffer samples (coreset) before inference violates the *single-pass learning constraint*. Moreover, it still does not outperform our approach even with the finetuning. More

details are given in the appendix.

REMIND [15] is a recently proposed rehearsal-based lifelong learning approach, which combats catastrophic forgetting in *online streaming setting*. While it follows a setting close to the one proposed, the model stores a large number of past examples compared to the other baselines; for example, iCaRL [34] stores 10K past examples for the ImageNet experiment, whereas REMIND stores 1M past examples. Further, it actually uses a lossy compression to store past samples, which is merely an engineering technique, not an algorithmic improvement, and can be used by any continual learning approach. For more details, please refer to the appendix.

## 5. Experiments

### 5.1. Baselines And Compared Methods

The proposed approach follows the ‘*online streaming setting*’; to the best of our knowledge, recent works ExStream [14] and REMIND [15] are the only methods that follow this setting. We compare our approach against these strong baselines. We also compare our model with (i) a network trained with a sample one at a time (Fine-tuning/lower-bound) and (ii) a network trained offline, assuming all the data is available (Offline/upper-bound). Also, for rigorous comparison, we choose recent popular ‘batch’ and ‘online’ continual learning methods, such as EWC [23], MAS [1], VCL with/without coreset [31], Coreset Only [10], TinyER [8], GDumb [33] and A-Gem [7]. For a fair comparison, we train all the methods in an online streaming setting, i.e., one sample at a time. ‘VCL w/ C/’ and ‘Coreset only’ are both trained in a streaming manner; however, the network is fine-tuned with the stored samples before inference. Also, GDumb stores samples in memory and fine-tunes the network with them before inference, while fine-tuning is prohibited in ‘*streaming setting*’. Therefore, VCL and GDumb have an extra advantage compared to the true ‘*streaming learning*’ approaches. Still, CIOSL outperforms these approaches by a significant margin. More details are given in the appendix.

### 5.2. Datasets, Data Orderings And Metrics

**Datasets.** To evaluate the efficacy of the proposed model we perform extensive experiments on four standard datasets: CIFAR10, CIFAR100 [24], ImageNet100, and iCubWorld-1.0 [9]. CIFAR10 and CIFAR100 are standard classification datasets with 10 and 100 classes, respectively. ImageNet100 is a subset of ImageNet-1000 (ILSVRC-2012) [36] containing randomly chosen 100 classes, with each class containing 700-1300 training samples and 50 validation samples, which are used for testing. iCubWorld 1.0 is an object recognition dataset which contains the sequences of video frames, with each containing a single object. There are 10 classes, with

Method	Learning				
	Type	Fine-tunes	V.C.SL	Regularize	Memory
EWC	Batch	✗	✗	✓	✗
MAS	Batch	✗	✗	✓	✗
VCL	Batch	✗	✗	✓	✗
VCL w/ C/	Batch	✓	✓	✓	✓
Coreset	Online	✓	✓	✗	✓
GDumb	Online	✓	✓	✗	✓
TinyER	Online	✗	✗	✗	✓
A-GEM	Online	✗	✗	✓	✓
ExStream	Streaming	✗	✗	✗	✓
REMIND	Streaming	✗	✗	✗	✓
<b>Ours</b>	Streaming	✗	✗	✓	✓

Table 1. Categorization of the baseline approaches depending on the underlying simplifying assumptions they impose. V.C.SL: Violates Constraints of Streaming Learning

each containing 3 different object instances with 200-201 images each. Overall, each class contains 600-602 samples for training and 200-201 samples for testing. Technically, iCubWorld 1.0 is ideal dataset for *streaming learning*, as it requires learning from temporally ordered image sequences, i.e., *non-i.i.d* images.

**Evaluation Over Different Data Orderings.** The proposed approach is robust to the various streaming learning setting; we evaluate the model’s streaming learning ability with the following four [14, 15] challenging data ordering schemes: (i) *‘streaming iid’*: where the data-stream is organized by the randomly shuffled samples from the dataset, (ii) *‘streaming class iid’*: where the data-stream is organized by the samples from one or more classes, these samples are shuffled randomly, (iii) *‘streaming instance’*: where the data-stream is organized by temporally ordered samples from different object instances, and (iv) *‘streaming class instance’*: where the data-stream is organized by the samples from different classes, the samples within a class are temporally ordered based on different object instances. Only iCubWorld dataset contains the temporal ordering therefore *‘streaming instance’*, and *‘streaming class instance’* setting evaluated only on the iCubWorld dataset. Please refer to the appendix for more details.

**Metrics.** For evaluating the performance of the streaming learner, we use  $\Omega_{\text{all}}$  metric, similar to [14, 15, 21], where  $\Omega_{\text{all}}$  represents normalized incremental learning performance with respect to an offline learner:  $\Omega_{\text{all}} = \frac{1}{T} \sum_{t=1}^T \frac{\alpha_t}{\alpha_{\text{offline},t}}$ , where  $T$  is the total number of testing events,  $\alpha_t$  is the performance of the incremental learner at time  $t$ , and  $\alpha_{\text{offline},t}$  is the performance of a traditional offline model at time  $t$ .

### 5.3. Implementation Details

In all the experiments, models are trained with one sample at a time. For a fair comparison, a similar network structure is used throughout all the models. For all methods, we use fully connected single-head networks with two hidden layers as the plastic network  $F(\cdot)$ , where each layer contains 256

nodes with ReLU activations; for ‘VCL w/ or w/o Coreset’, ‘Coreset only’ and ‘CIOSL’,  $F(\cdot)$  is a BNN, whereas for all other methods  $F(\cdot)$  is a deterministic network. For a fair comparison, we store the same number of past examples for all replay-based approaches. For REMIND, we compress and store the feature-maps with Faiss [19] product quantization (PQ) implementation with  $s = 32$  sub-vectors and codebook size  $c = 256$ .

We store the feature-map in memory for all the other methods, including our approach CIOSL. In addition, CIOSL also store the corresponding logits, loss-values, and uncertainty-scores. The capacity of our replay buffer is mentioned in Table 3. For memory-replay, we use *‘uncertainty-aware positive-negative’* sampling strategy (discussed in Sec:3.2) throughout all data-orderings, except for *‘streaming-i.i.d’* ordering, we use *‘uniform’* sampling. We use *‘loss-aware weighted random replacement with a reservoir’* sampling strategy as memory replacement policy for all the experiments. We store the same number of past examples in memory across all methods. For memory-replay, we use  $N'_1 = 16$  past samples throughout all experiments across CIOSL, AGEM, TinyER, ExStream and REMIND. For knowledge-distillation, CIOSL use  $N'_2 = 16$  samples at any time step  $t$ . We set the hyper-parameter  $\lambda_1 = 1$  and  $\lambda_2 = 0.3$  across all experiments. For EWC, we set hyper-parameter  $\lambda = 500$ , and for MAS, we set hyper-parameter  $\lambda = 1$ . We repeated each experiments for 10 times with different permutations of the data, and reported the results by taking average of 10 runs. Please refer to the appendix for more details.

### 5.4. Results

The detailed results of CIOSL over various experimental settings along with the strong baseline methods are shown in Table 2. We can clearly observe that CIOSL consistently outperforms the baseline by a significant margin. The proposed model is also robust to the different streaming learning scenarios compared to the baselines. We repeat our experiment ten times, because of the space constraint, we omit standard-deviations and included in the appendix. We do not consider GDumb as the best-performing method, even when it achieves higher accuracy for the class-iid since it finetunes the network with the stored samples and makes the learning algorithm a *‘two-step’* process, which is prohibited in *streaming-learning*. We observe that ‘batch-learning’ methods severely suffer from catastrophic forgetting. Moreover, replay-based ‘online-learning’ method such as AGEM also suffer from information loss badly. Furthermore, GDumb, even with finetuning before each inference, cannot achieve the best accuracy in all the experiments. CIFAR10/100, ImageNet are the standard classification datasets, while iCubWorld 1.0 is a challenging dataset that evaluates the models in more realistic scenarios or data-orderings. Particularly,

Method	iid				Class-iid				Instance	Class-instance
	CIFAR10	CIFAR100	ImageNet100	iCubWorld	CIFAR10	CIFAR100	ImageNet100	iCubWorld	iCubWorld	iCubWorld
Fine-Tune	0.1175	0.0180	0.0127	0.1369	0.3447	0.1277	0.1223	0.3893	0.1307	0.3485
EWC	-	-	-	-	0.3446	0.1292	0.1225	0.3790	-	0.3487
MAS	-	-	-	-	0.3470	0.1280	0.1234	0.3912	-	0.3486
VCL	-	-	-	-	0.3442	0.1273	0.1205	0.3806	-	0.3473
VCL w/ C/	-	-	-	-	0.3716	0.1414	0.1259	0.3948	-	0.4705
Coreset	-	-	-	-	0.3684	0.1432	0.1273	0.3994	-	0.4669
<b>GDumb</b>	0.8686	0.6067	0.8361	0.8993	<b>0.9252</b>	0.7635	<b>0.9197</b>	<b>0.9660</b>	0.6715	0.7908
A-GEM	0.1175	0.0182	0.0139	0.1311	0.3448	0.1290	0.1215	0.4047	0.1309	0.3489
TinyER	0.9314	0.7588	0.9415	0.9590	0.8926	0.7402	0.8995	0.9069	0.8726	0.8215
ExStream	0.8866	0.7845	0.9293	0.9235	0.8123	0.7176	0.8757	0.8820	0.8954	0.8727
REMIND	0.8910	0.6457	0.9088	0.9260	0.8832	0.6787	0.8803	0.8553	0.8157	0.7615
<b>Ours</b>	<b>0.9579</b>	<b>0.8679</b>	<b>0.9640</b>	<b>0.9716</b>	<b>0.8991</b>	<b>0.7724</b>	<b>0.9171</b>	<b>0.9480</b>	<b>0.9580</b>	<b>0.9585</b>
Offline	1.0000	1.0000	1.0000	1.0000	1.0000	1.0000	1.0000	1.0000	1.0000	1.0000
Offline	0.8509	0.6083	0.8520	0.7626	0.8972	0.7154	0.8953	0.8849	0.7646	0.8840

Table 2.  $\Omega_{\text{all}}$  results. For each experiment, the method with best performance in ‘streaming-setting’ is highlighted in **Bold**. The reported results are average over 10 runs with different permutations of the data. Offline model is trained only once.  $\widehat{\text{Offline}} = \frac{1}{T} \sum_{t=1}^T \alpha_{\text{offline},t}$ , where  $T$  is the total number of testing events. ‘-’ indicates experiments we were unable to run, because of compatibility issues. Methods in **Red** use fine-tuning before inference, which violates ‘single-pass’ learning constraint.

Dataset	CIFAR10	CIFAR100	ImageNet100	iCubWorld 1.0
Buffer Capacity	1000	1000	1000	180
Training-Set Size	50000	50000	127778	6002

Table 3. Memory buffer capacity used for various datasets.

class-instance ordering and instance ordering require the learner to learn from temporally ordered video frames one at a time. From Table 2, we observe that CIOSSL obtain up to **8.58%** and **6.26%** improvement over the state-of-the-art streaming learning approaches. In fact, in most of the scenarios, CIOSSL is very close to the upper bound performance, i.e., when the model is trained in a fully offline fashion.

For completeness, we train ‘Our-method’ in ‘batch’ and ‘online’ learning setting to determine its effectiveness and compatibility in these settings. In Figure 1, we compare  $\Omega_{\text{all}}$  results of various baseline with our-method CIOSSL. We observe that CIOSSL outperforms the baselines by a significant margin on both class-i.i.d and class-instance ordering on iCubWorld 1.0 dataset. This implies that a method trained in the extreme setting can be thought of as a universal method for all *lifelong learning settings* with the widest possible applicability. More details are given in the appendix.

## 6. Ablation Study

We perform extensive ablation to show the importance of the different components. The various ablation experiments validate the significance of the proposed components.

**Significance Of Different Sampling Strategies.** In Table 4, we compare the performance of CIOSSL while using various sampling strategies and memory replacement policies. We observe that for the buffer replacement, LAWRRR

performs better compared to LAWCBR. Furthermore, for the sample replay, UAPN, along with LAWRRR memory buffer policy, outperforms other sampling strategies, except *uniform sampling* (Uni) performs better on i.i.d ordering. We provide more details in the appendix.

Memory Replacement	Sample Selection	iCubWrold		ImageNet100	
		instance	Class instance	iid	Class-iid
LAWCBR	Uni	0.8975	0.8506	0.9582	0.9014
	UAPN	0.9346	0.8500	0.9327	0.9135
	LAPN	0.9172	0.8536	0.9253	0.9122
LAWRRR	Uni	0.9269	0.9346	<b>0.9640</b>	0.8643
	UAPN	<b>0.9580</b>	<b>0.9585</b>	0.9578	<b>0.9171</b>
	LAPN	0.9558	0.9497	0.9575	0.9112

Table 4.  $\Omega_{\text{all}}$  Results. For each experiment, the method with best performance is highlighted in **Bold**.

**Choice Of Hyperparameter ( $\lambda_2$ ).** Figure 4 shows the effect of changing the knowledge-distillation loss weight  $\lambda_2$  on the final  $\Omega_{\text{all}}$  accuracy for iCubWorld 1.0 on instance and class-instance ordering, while using different sampling strategies and buffer replacement policies. We observe the best model performance for  $\lambda_2 = 0.3$ , and we use this value of  $\lambda_2$  for all our experiments. We provide detailed ablation on  $\lambda_2$  in the appendix.

**Significance Of Knowledge-Distillation Loss.** Figure 4 with  $\lambda_2 = 0.0$  represents the model without knowledge distillation. We can observe that the model performance significantly degrades without knowledge distillation. Therefore, knowledge distillation is a key component to the model’s performance. More details are given in the appendix.

**Choice Of Buffer Capacity.** We perform an ablation for the different buffer capacities, i.e.,  $|\mathcal{M}|$ . The results are shown in Figure 5. It is evident that, with the longer se-

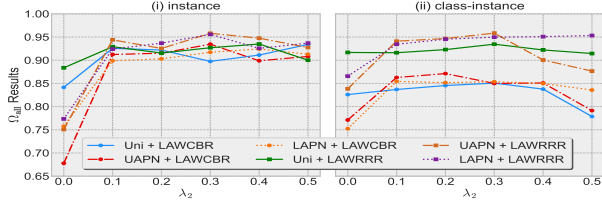


Figure 4. Plots of  $\Omega_{\text{all}}$  as a function of hyper-parameter  $\lambda_2$  and different sampling strategies and replacement policies for (i) instance, (ii) class-instance ordering on iCubWorld 1.0.

quence of incoming data, the model’s (CIOSL) performance improves with the increase in the buffer capacity, as it helps minimize the confusion in the output prediction.

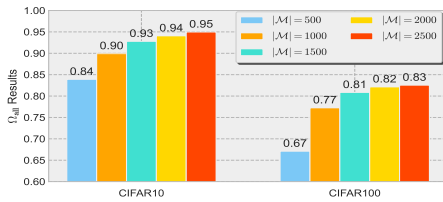


Figure 5. Plots of  $\Omega_{\text{all}}$  as a function of buffer capacity  $|\mathcal{M}|$  for class-i.i.d data-ordering on CIFAR10 and CIFAR100.

## 7. Conclusion

*Streaming continual learning* (SCL) is the most challenging and realistic framework for continual learning; most of the recent promising models for the CL are unable to handle this above setting. Our work proposes a dual regularization and loss-aware sample replay to handle the SCL scenario. The proposed model is highly efficient since it learns a joint likelihood from the current and replay samples without leveraging any external finetuning. Also, to improve the training efficiency further, the proposed model selects a few most informative samples from the buffer instead of using the entire buffer for the replay. We have conducted a rigorous experiment over several challenging datasets and showed that CIOSL outperforms state-of-the-art approaches in this setting by a significant margin. To disentangle the importance of the various components, we perform extensive ablation studies and observe that the proposed components are essential to handle the SCL setting.

## References

- [1] Rahaf Aljundi, Francesca Babiloni, Mohamed Elhoseiny, Marcus Rohrbach, and Tinne Tuytelaars. Memory aware synapses: Learning what (not) to forget. In *Proceedings of the European Conference on Computer Vision (ECCV)*, pages 139–154, 2018. 1, 2, 5, 10, 12
- [2] Rahaf Aljundi, Marcus Rohrbach, and Tinne Tuytelaars. Selfless sequential learning. *arXiv preprint arXiv:1806.05421*, 2018. 10
- [3] Charles Blundell, Julien Cornebise, Koray Kavukcuoglu, and Daan Wierstra. Weight uncertainty in neural networks. *arXiv preprint arXiv:1505.05424*, 2015. 3, 10
- [4] Pietro Buzzega, Matteo Boschini, Angelo Porrello, Davide Abati, and Simone Calderara. Dark experience for general continual learning: a strong, simple baseline. *arXiv preprint arXiv:2004.07211*, 2020. 5
- [5] Lucy R Chai. Uncertainty estimation in bayesian neural networks and links to interpretability. *Master of Philosophy (University of Cambridge)*, 2018. 4
- [6] Arslan Chaudhry, Puneet K Dokania, Thalaiyasingam Ajanthan, and Philip HS Torr. Riemannian walk for incremental learning: Understanding forgetting and intransigence. In *Proceedings of the European Conference on Computer Vision (ECCV)*, pages 532–547, 2018. 10
- [7] Arslan Chaudhry, Marc’Aurelio Ranzato, Marcus Rohrbach, and Mohamed Elhoseiny. Efficient lifelong learning with a-gem. *arXiv preprint arXiv:1812.00420*, 2018. 1, 5, 12
- [8] Arslan Chaudhry, Marcus Rohrbach, Mohamed Elhoseiny, Thalaiyasingam Ajanthan, Puneet K Dokania, Philip HS Torr, and M Ranzato. Continual learning with tiny episodic memories. 2019. 5, 12
- [9] Sean Fanello, Carlo Ciliberto, Matteo Santoro, Lorenzo Natale, Giorgio Metta, Lorenzo Rosasco, and Francesca Odone. icub world: Friendly robots help building good vision datasets. In *Proceedings of the IEEE Conference on Computer Vision and Pattern Recognition Workshops*, pages 700–705, 2013. 5, 13, 15, 17
- [10] Sebastian Farquhar and Yarin Gal. Towards robust evaluations of continual learning. *arXiv preprint arXiv:1805.09733*, 2018. 5, 10, 12
- [11] Chrisantha Fernando, Dylan Banarse, Charles Blundell, Yori Zwols, David Ha, Andrei A Rusu, Alexander Pritzel, and Daan Wierstra. Pathnet: Evolution channels gradient descent in super neural networks. *arXiv preprint arXiv:1701.08734*, 2017. 5
- [12] Robert M French. Catastrophic forgetting in connectionist networks. *Trends in cognitive sciences*, 3(4):128–135, 1999. 1, 10, 13, 15
- [13] Soumya Ghosh, Jiayu Yao, and Finale Doshi-Velez. Structured variational learning of bayesian neural networks with horseshoe priors. In *International Conference on Machine Learning*, pages 1744–1753. PMLR, 2018. 3
- [14] Tyler L Hayes, Nathan D Cahill, and Christopher Kanan. Memory efficient experience replay for streaming learning. In *2019 International Conference on Robotics and Automation (ICRA)*, pages 9769–9776. IEEE, 2019. 1, 2, 5, 6, 10, 11, 12, 13
- [15] Tyler L Hayes, Kushal Kafle, Robik Shrestha, Manoj Acharya, and Christopher Kanan. Remind your neural network to prevent catastrophic forgetting. *arXiv preprint arXiv:1910.02509*, 2019. 1, 5, 6, 10, 11, 13
- [16] Geoffrey Hinton, Oriol Vinyals, and Jeff Dean. Distilling the knowledge in a neural network. *arXiv preprint arXiv:1503.02531*, 2015. 4, 5

- [17] David Isele and Akansel Cosgun. Selective experience replay for lifelong learning. *arXiv preprint arXiv:1802.10269*, 2018. [5](#)
- [18] Herve Jegou, Matthijs Douze, and Cordelia Schmid. Product quantization for nearest neighbor search. *IEEE transactions on pattern analysis and machine intelligence*, 33(1):117–128, 2010. [10](#)
- [19] Jeff Johnson, Matthijs Douze, and Hervé Jégou. Billion-scale similarity search with gpus. *IEEE Transactions on Big Data*, 2019. [6](#)
- [20] Ronald Kemker and Christopher Kanan. Fearnert: Brain-inspired model for incremental learning. *arXiv preprint arXiv:1711.10563*, 2017. [5](#)
- [21] Ronald Kemker, Marc McClure, Angelina Abitino, Tyler L Hayes, and Christopher Kanan. Measuring catastrophic forgetting in neural networks. In *Thirty-second AAAI conference on artificial intelligence*, 2018. [6](#)
- [22] Diederik P Kingma and Max Welling. Auto-encoding variational bayes. *arXiv preprint arXiv:1312.6114*, 2013. [10](#)
- [23] James Kirkpatrick, Razvan Pascanu, Neil Rabinowitz, Joel Veness, Guillaume Desjardins, Andrei A Rusu, Kieran Milan, John Quan, Tiago Ramalho, Agnieszka Grabska-Barwinska, et al. Overcoming catastrophic forgetting in neural networks. *Proceedings of the national academy of sciences*, 114(13):3521–3526, 2017. [1](#), [2](#), [5](#), [10](#), [12](#)
- [24] Alex Krizhevsky, Geoffrey Hinton, et al. Learning multiple layers of features from tiny images. 2009. [5](#), [14](#)
- [25] Alex Krizhevsky, Ilya Sutskever, and Geoffrey E Hinton. Imagenet classification with deep convolutional neural networks. In *Advances in neural information processing systems*, pages 1097–1105, 2012. [5](#)
- [26] Sang-Woo Lee, Jin-Hwa Kim, Jaehyun Jun, Jung-Woo Ha, and Byoung-Tak Zhang. Overcoming catastrophic forgetting by incremental moment matching. In *Advances in neural information processing systems*, pages 4652–4662, 2017. [5](#)
- [27] Zhizhong Li and Derek Hoiem. Learning without forgetting. *IEEE transactions on pattern analysis and machine intelligence*, 40(12):2935–2947, 2017. [5](#)
- [28] Arun Mallya, Dillon Davis, and Svetlana Lazebnik. Piggyback: Adapting a single network to multiple tasks by learning to mask weights. In *Proceedings of the European Conference on Computer Vision (ECCV)*, pages 67–82, 2018. [5](#)
- [29] Arun Mallya and Svetlana Lazebnik. Packnet: Adding multiple tasks to a single network by iterative pruning. In *Proceedings of the IEEE Conference on Computer Vision and Pattern Recognition*, pages 7765–7773, 2018. [5](#)
- [30] Radford M Neal. *Bayesian learning for neural networks*, volume 118. Springer Science & Business Media, 2012. [3](#), [10](#)
- [31] Cuong V Nguyen, Yingzhen Li, Thang D Bui, and Richard E Turner. Variational continual learning. *arXiv preprint arXiv:1710.10628*, 2017. [1](#), [3](#), [5](#), [10](#), [12](#)
- [32] Adam Paszke, Sam Gross, Francisco Massa, Adam Lerer, James Bradbury, Gregory Chanan, Trevor Killeen, Zeming Lin, Natalia Gimelshein, Luca Antiga, et al. Pytorch: An imperative style, high-performance deep learning library. In *Advances in neural information processing systems*, pages 8026–8037, 2019. [13](#)
- [33] Ameya Prabhu, Philip HS Torr, and Puneet K Dokania. Gdumb: A simple approach that questions our progress in continual learning. In *European Conference on Computer Vision*, pages 524–540. Springer, 2020. [1](#), [2](#), [5](#), [12](#)
- [34] Sylvestre-Alvise Rebuffi, Alexander Kolesnikov, Georg Sperl, and Christoph H Lampert. icarl: Incremental classifier and representation learning. In *Proceedings of the IEEE conference on Computer Vision and Pattern Recognition*, pages 2001–2010, 2017. [5](#), [10](#)
- [35] Amanda Rios and Laurent Itti. Closed-loop memory gan for continual learning. *arXiv preprint arXiv:1811.01146*, 2018. [5](#)
- [36] Olga Russakovsky, Jia Deng, Hao Su, Jonathan Krause, Sanjeev Satheesh, Sean Ma, Zhiheng Huang, Andrej Karpathy, Aditya Khosla, Michael Bernstein, et al. Imagenet large scale visual recognition challenge. *International journal of computer vision*, 115(3):211–252, 2015. [5](#), [13](#), [14](#), [17](#)
- [37] Andrei A Rusu, Neil C Rabinowitz, Guillaume Desjardins, Hubert Soyer, James Kirkpatrick, Koray Kavukcuoglu, Razvan Pascanu, and Raia Hadsell. Progressive neural networks. *arXiv preprint arXiv:1606.04671*, 2016. [1](#), [5](#)
- [38] Mark Sandler, Andrew Howard, Menglong Zhu, Andrey Zhmoginov, and Liang-Chieh Chen. Mobilenetv2: Inverted residuals and linear bottlenecks. In *Proceedings of the IEEE conference on computer vision and pattern recognition*, pages 4510–4520, 2018. [5](#), [13](#)
- [39] Joan Serra, Didac Suris, Marius Miron, and Alexandros Karatzoglou. Overcoming catastrophic forgetting with hard attention to the task. *arXiv preprint arXiv:1801.01423*, 2018. [5](#)
- [40] Hanul Shin, Jung Kwon Lee, Jaehong Kim, and Jiwon Kim. Continual learning with deep generative replay. In *Advances in Neural Information Processing Systems*, pages 2990–2999, 2017. [1](#), [5](#)
- [41] Jeffrey S Vitter. Random sampling with a reservoir. *ACM Transactions on Mathematical Software (TOMS)*, 11(1):37–57, 1985. [4](#)
- [42] Chenshen Wu, Luis Herranz, Xialei Liu, Joost van de Weijer, Bogdan Raducanu, et al. Memory replay gans: Learning to generate new categories without forgetting. In *Advances In Neural Information Processing Systems*, pages 5962–5972, 2018. [1](#), [5](#)
- [43] Ye Xiang, Ying Fu, Pan Ji, and Hua Huang. Incremental learning using conditional adversarial networks. In *Proceedings of the IEEE International Conference on Computer Vision*, pages 6619–6628, 2019. [5](#)
- [44] Jaehong Yoon, Eunho Yang, Jeongtae Lee, and Sung Ju Hwang. Lifelong learning with dynamically expandable networks. *arXiv preprint arXiv:1708.01547*, 2017. [5](#)
- [45] Jason Yosinski, Jeff Clune, Yoshua Bengio, and Hod Lipson. How transferable are features in deep neural networks? In *Advances in neural information processing systems*, pages 3320–3328, 2014. [5](#)
- [46] Fei Zhu, Xu-Yao Zhang, Chuang Wang, Fei Yin, and Cheng-Lin Liu. Prototype augmentation and self-supervision for incremental learning. In *Proceedings of the IEEE/CVF Conference on Computer Vision and Pattern Recognition*, pages 5871–5880, 2021. [5](#)

## A. Preliminaries

### A.1. ‘Class Incremental Learning’ V/S ‘Task Incremental/Multi-Task Learning’

‘Class incremental learning’ [6, 14, 15, 34], is a challenging variant of lifelong learning, where the classifier needs to learn to discriminate between different class labels from different tasks. The key distinction between ‘class incremental learning’ and ‘task incremental/multi-task learning’ [1, 2, 23, 31], lies in how the classifier’s accuracy is evaluated at the test time. In ‘class incremental learning’, at the test time, the task identifier  $t$  is not specified, and the accuracy is computed over all the observed classes with  $\frac{1}{\mathcal{C}}$  chance, where  $\mathcal{C}$  is the total number of classes accumulated so far. However, in ‘task incremental learning’, the task identifier  $t$  is known.

For example, consider MNIST divided into 5 tasks:  $\{\{0, 1\}, \dots, \{8, 9\}\}$ , which are used for sequential learning of a classifier. Then, at the end of 5-th task, in ‘task incremental setting’, the classifier needs to predict a class out of  $\{8, 9\}$  only. However, in ‘class incremental setting’, a class label is predicted over all the ten classes that is observed so far, i.e.,  $\{0, \dots, 9\}$  with  $\frac{1}{10}$  chance for each class.

### A.2. Variational Continual Learning (VCL)

Variational Continual Learning (VCL) [31] is a recently proposed continual learning approach that mitigates catastrophic forgetting in neural networks in a Bayesian framework. It sets the posterior of parameters distribution as the prior before training on the next task, i.e.,  $p_t(\theta) = q_{t-1}(\theta)$ , the new task reuses the previous task’s posterior as the new prior. VCL solves the following KL divergence minimization problem while training on task  $t$  with the new data  $\mathcal{D}_t$ :

$$q_t(\theta) = \arg \min_{q \in \mathcal{Q}} \text{KL} \left( q(\theta) \parallel \frac{1}{Z_t} q_{t-1}(\theta) p(\mathcal{D}_t | \theta) \right) \quad (7)$$

While offering a principled way of continual learning, VCL follows *task incremental / multi task learning* setting, and uses ‘task specific head networks’, for each task  $t$ , such that,  $p(\theta | \mathcal{D}_{1:t}) = p(\theta_t | \mathcal{D}_t) p(\theta_S | \mathcal{D}_{1:t})$ , where  $\theta = \{\theta_S, \theta_t\}$ ,  $\theta_S$  is shared between all the tasks, whereas  $\theta_t$  kept fixed after training on task  $t$ . This configuration prohibits knowledge transfer across tasks, and results in a poor accuracy in *class incremental setting* [10] for both VCL with or without Coreset.

VCL with Coreset [31] withheld some data points from the task data before training and keeps them in a coreset. These data points are not used for the network training and are only used for finetuning the network before each inference. However, in *online streaming learning* finetuning the network at any time is prohibited, as it makes the training process a *two-step* learning process instead of *single-pass* learning. Furthermore, the coreset is created by sampling data

points from the entire task data, whereas in *online streaming setting*, each instance arrives one at a time. Finally, the performance of *VCL with Coreset* is heavily dependent on the finetuning with the withheld samples, i.e., coreset samples, before inference [10], and still not comparable enough to our proposed method (CIOSL).

### A.3. REMIND

REMIND [15] is a recently proposed replay-based lifelong learning approach which combats catastrophic forgetting [12] in deep neural network in *online-streaming setting*. While following such a challenging setting, it separates the convolutional neural network into two networks: (i) a frozen feature extractor and (ii) a plastic neural network. Learning involves the following steps: (i) compression of each new input using product quantization (PQ) [18], (ii) reconstruction of the previously stored compressed representations using PQ, and (iii) mixing the reconstructed past examples with the new input and updating the parameters of the plastic layers of the network.

While it offers a principled way to combat catastrophic forgetting and achieves state-of-the-art performance, there are few concerns that can be limiting in the continual learning setup. It stores considerably a large number of past examples compared to the baselines; for example, iCaRL [34] stores 10K past examples for ImageNet experiment whereas REMIND stores 1M past examples. Furthermore, REMIND actually uses a lossy compression method (PQ) to store the past samples, which is merely an engineering technique far from any algorithmic improvement and can be used by any lifelong learning approach.

### A.4. Bayesian Neural Network

Bayesian neural networks [30] are discriminative models, which extend the standard deep neural networks with Bayesian inference. The network parameters are assumed to have a prior distribution,  $p(\theta)$ , and it infers the posterior given the observed data  $\mathcal{D}$ , that is,  $p(\theta | \mathcal{D})$ . However, the exact posterior inference is computationally intractable for any complex models, and an approximation is needed. One such scheme is ‘*Bayes-by-Backprop*’ [3]. It uses a mean-field variational posterior  $q(\theta)$  over the network parameters and uses reparameterization-trick [22] to sample from the posterior, which are then used to approximate the evidence lower bound (ELBO) via Monte-Carlo sampling.

In our proposed method (CIOSL), we have used a Bayesian neural network (BNN) as the plastic network  $F(\cdot)$ . We have discussed training the plastic network (BNN)  $F(\cdot)$  with a single step posterior update without catastrophic forgetting [12] in Section 3.1 in the main paper.

Method	iCubWorld 1.0					
	class-iid			class-instance		
	Batch	Online	Streaming	Batch	Online	Streaming
VCL	0.5493 ± 0.0372	0.4835 ± 0.0132	0.3806 ± 0.0527	0.3299 ± 0.0469	0.3469 ± 0.0031	0.3473 ± 0.0025
VCL w/ C/	0.5314 ± 0.0306	0.4849 ± 0.0093	0.3948 ± 0.0558	0.4353 ± 0.0354	0.4373 ± 0.0284	0.4705 ± 0.0165
A-GEM	-	0.4890 ± 0.0063	0.4047 ± 0.0632	-	0.3497 ± 0.0013	0.3489 ± 0.0030
TinyER	0.9109 ± 0.0241	0.8382 ± 0.0332	0.9069 ± 0.0297	0.8106 ± 0.0486	0.7042 ± 0.0526	0.8215 ± 0.0341
REMIND	0.8381 ± 0.0333	0.6525 ± 0.0426	0.8553 ± 0.0349	0.6170 ± 0.0930	0.5879 ± 0.0473	0.7615 ± 0.0319
<b>Ours</b>	<b>0.9585 ± 0.0184</b>	<b>0.8969 ± 0.0320</b>	<b>0.9480 ± 0.0215</b>	<b>0.8769 ± 0.0647</b>	<b>0.8300 ± 0.0587</b>	<b>0.9585 ± 0.0223</b>

Table 5.  $\Omega_{\text{all}}$  with their associated standard deviations for ‘batch’, ‘online’, and ‘streaming’ versions of baselines on iCubWorld 1.0 on (*i*) class-i.i.d, and (*ii*) class-instance ordering. ‘-’ indicates experiments we were unable to run, because of compatibility issues.

Method	iid			Class-iid		
	CIFAR10	CIFAR100	ImageNet100	CIFAR10	CIFAR100	ImageNet100
Fine-Tune	0.1175 ± 0.0000	0.0180 ± 0.0035	0.0127 ± 0.0029	0.3447 ± 0.0003	0.1277 ± 0.0022	0.1223 ± 0.0052
EWC	-	-	-	0.3446 ± 0.0003	0.1292 ± 0.0037	0.1225 ± 0.0039
MAS	-	-	-	0.3470 ± 0.0075	0.1280 ± 0.0029	0.1234 ± 0.0046
VCL	-	-	-	0.3442 ± 0.0006	0.1273 ± 0.0041	0.1205 ± 0.0015
VCL w/ C/	-	-	-	0.3716 ± 0.0501	0.1414 ± 0.0224	0.1259 ± 0.0122
Coreset	-	-	-	0.3684 ± 0.0442	0.1432 ± 0.0256	0.1273 ± 0.0182
GDumb	0.8686 ± 0.0065	0.6067 ± 0.0119	0.8361 ± 0.0070	<b>0.9252 ± 0.0057</b>	0.7635 ± 0.0096	<b>0.9197 ± 0.0081</b>
A-GEM	0.1175 ± 0.0000	0.0182 ± 0.0035	0.0139 ± 0.0041	0.3448 ± 0.0002	0.1290 ± 0.0037	0.1215 ± 0.0025
TinyER	0.9314 ± 0.0114	0.7588 ± 0.0128	0.9415 ± 0.0085	0.8926 ± 0.0158	0.7402 ± 0.0195	0.8995 ± 0.0122
ExStream	0.8866 ± 0.0244	0.7845 ± 0.0121	0.9293 ± 0.0082	0.8123 ± 0.0209	0.7176 ± 0.0208	0.8757 ± 0.0148
REMIND	0.8910 ± 0.0073	0.6457 ± 0.0091	0.9088 ± 0.0109	0.8832 ± 0.0201	0.6787 ± 0.0215	0.8803 ± 0.0157
<b>Ours</b>	<b>0.9579 ± 0.0040</b>	<b>0.8679 ± 0.0057</b>	<b>0.9640 ± 0.0060</b>	<b>0.8991 ± 0.0089</b>	<b>0.7724 ± 0.0188</b>	<b>0.9171 ± 0.0073</b>
Offline	1.0000	1.0000	1.0000	1.0000	1.0000	1.0000
$\overline{\text{Offline}}$	0.8509	0.6083	0.8520	0.8972	0.7154	0.8953

Table 6.  $\Omega_{\text{all}}$  results with their associated standard deviations. For each experiment, the method with best performance in ‘streaming-setting’ is highlighted in **Bold**. The reported results are average over 10 runs with different permutations of the data. Offline model is trained only once.  $\overline{\text{Offline}} = \frac{1}{T} \sum_{t=1}^T \alpha_{\text{offline},t}$ , where  $T$  is the total number of testing events. ‘-’ indicates experiments we were unable to run, because of compatibility issues. Methods in **Red** use fine-tuning before inference, which violates ‘single-pass’ learning constraint.

## B. $\Omega_{\text{all}}$ Results With Their Associated Standard Deviations

We repeated each experiment 10 times with different permutations of the data and reported the results by taking the average over 10 runs. However, due to space constraint, we could not include the  $\Omega_{\text{all}}$  results with their associated standard deviations in the main paper, which we provide here.

In Table 5, we provide the detailed results (corresponding Figure 1 of main paper) with their associated standard deviations comparing CIOSL and other baselines in different learning settings. It empirically shows that CIOSL which is designed considering the extreme and most restrictive *online streaming setting* can be thought of as a universal lifelong learning method with the widest possible applicability.

Table 6 and Table 7 provides the detailed results (main paper Table 2) of CIOSL with their associated standard deviations over various experimental settings along with the

state-of-the-art baselines. We observe that CIOSL is the best performing method throughout all the experiments. Particularly, in the challenging scenarios such as class-instance and instance ordering where the model needs to learn from temporally ordered image sequence, the proposed approach (CIOSL) achieves **8.58%** and **6.26%** improvement over the state-of-the-art baselines.

## C. Baselines And Compared Methods In Detail

The proposed approach (CIOSL) follows ‘*online streaming setting*’, to the best of our knowledge, recent works ExStream [14], and REMIND [15] are the only method that trains a *deep neural network* following our setting. We compared our approach (CIOSL) against these strong baselines. In addition, we have compared various ‘batch’ and ‘online’ learning methods, which we describe below.

For a fair comparison, we follow a similar network structure throughout all the methods. We separate a convolutional

Method	iCubWorld 1.0			
	iid	Class-iid	Instance	Class-instance
Fine-Tune	0.1369 ± 0.0184	0.3893 ± 0.0534	0.1307 ± 0.0000	0.3485 ± 0.0022
EWC	-	0.3790 ± 0.0419	-	0.3487 ± 0.0034
MAS	-	0.3912 ± 0.0613	-	0.3486 ± 0.0019
VCL	-	0.3806 ± 0.0527	-	0.3473 ± 0.0025
VCL w/ C/	-	0.3948 ± 0.0558	-	0.4705 ± 0.0165
Coreset	-	0.3994 ± 0.0922	-	0.4669 ± 0.0251
GDumb	0.8993 ± 0.0413	<b>0.9660 ± 0.0201</b>	0.6715 ± 0.0540	0.7908 ± 0.0329
A-GEM	0.1311 ± 0.0000	0.4047 ± 0.0632	0.1309 ± 0.0003	0.3489 ± 0.0030
TinyER	0.9590 ± 0.0378	0.9069 ± 0.0297	0.8726 ± 0.0649	0.8215 ± 0.0341
ExStream	0.9235 ± 0.0584	0.8820 ± 0.0285	0.8954 ± 0.0542	0.8727 ± 0.0229
REMIND	0.9260 ± 0.0311	0.8553 ± 0.0349	0.8157 ± 0.0600	0.7615 ± 0.0319
<b>Ours</b>	<b>0.9716 ± 0.0141</b>	<b>0.9480 ± 0.0215</b>	<b>0.9580 ± 0.0298</b>	<b>0.9585 ± 0.0223</b>
Offline	1.0000	1.0000	1.0000	1.0000
$\widehat{\text{Offline}}$	0.7626	0.8849	0.7646	0.8840

Table 7.  $\Omega_{\text{all}}$  results with their associated standard deviations. For each experiment, the method with best performance in ‘streaming-setting’ is highlighted in **Bold**. The reported results are average over 10 runs with different permutations of the data. Offline model is trained only once.  $\widehat{\text{Offline}} = \frac{1}{T} \sum_{t=1}^T \alpha_{\text{offline},t}$ , where  $T$  is the total number of testing events. ‘-’ indicates experiments we were unable to run, because of compatibility issues. Methods in **Red** use fine-tuning before inference, which violates ‘single-pass’ learning constraint.

neural network (CNN) into two networks: (i) *non-plastic* feature extractor  $G(\cdot)$ , and (ii) *plastic* neural network  $F(\cdot)$ . For a given input image  $x$ , the predicted class label is computed as:  $y = F(G(x))$ . Across all the methods, we use the same initialization step for the feature extractor  $G(\cdot)$  (discussed in Section 3.5 in the main paper) and keep it frozen throughout the *streaming learning*. For all the methods, only the plastic network  $F(\cdot)$  is trained with one sample at a time in *streaming manner*. For details on the structure of the plastic network  $F(\cdot)$  across baselines along with CIOSL, please refer to Section 5.3 in the main paper.

In the below, we describe the baselines which we have evaluated along with our proposed method (CIOSL) in *online streaming setting*:

1. **EWC [23]**: It is a regularization-based incremental learning method, which penalizes any changes to the network parameters by the important weight measure, the diagonal of the Fisher information matrix.
2. **MAS [1]**: It is another regularization-based lifelong learning method, where the importance weight of the network parameters are estimated by measuring the magnitude of the gradient of the learned function.
3. **VCL [31]**: It uses variational inference (VI) with a Bayesian neural network to mitigate catastrophic forgetting, where it uses the previously learned posterior as the prior while learning incrementally with the sequentially coming data. For more details, please refer to Section A.2.
4. **VCL with Coreset [31]**: This method is the same as pure VCL as mentioned above, except, at the end of training on each task, the network is finetuned with the coreset samples. We adapted the coreset selection in *online streaming setting* and stored data points in coreset in an *online manner*.
5. **Coreset Only [10]**: This method is exactly similar to *VCL with Coreset [31]*, except the prior which is used for variational inference is the initial prior each time, i.e., it is not updated with the previous posterior before training on a new task.
6. **GDumb [33]**: It is an *online learning* method. It stores data points with a greedy sampler and retrains the network from scratch each time with stored samples before inference.
7. **A-Gem [7]**: It is another *online learning* approach. It uses past task data stored in memory to build an optimization constraint to be satisfied by each new update. If the gradient violates the constraint, then it is projected such that the constraint is satisfied.
8. **TinyER [8]**: It stores past task data points in a tiny episodic memory and replays them with the current training data to enable continual learning.
9. **ExStream [14]**: It is an *online streaming learning* method, which uses memory replay to enable continual learning. It maintains buffers of prototypes to store the input vectors. Once the buffer is full, it combines the

two nearest prototypes in the buffer and stores the new input vector.

10. **REMINd** [15]: Similar to ExStream, it is another *streaming learning* method, which enables lifelong learning with memory replay. For more details on REMIND, please refer to Section A.3.
11. **Fine-tuning**: It is a streaming learning baseline and serves as the lower bound on the network’s performance. In this scenario, the network parameters are fine-tuned with one instance through the whole dataset for a single epoch.
12. **Offline**: It serves as the upper bound on the network’s performance, where the network is trained in the traditional way; the complete dataset is divided into multiple batches, and the network loops over them multiple times.

**Note:** In *online streaming setting*, finetuning the network with the stored samples is prohibited, as it violates the *single-pass* learning constraint. ‘VCL with Coreset’, ‘Coreset Only’, and ‘GDumb’ finetune the network parameters before inference; therefore, these methods have an extra advantage compared to true *streaming learning* approaches, and they violate the *single-pass* learning constraint. Therefore these methods cannot be considered as the best-performing methods even when they achieve better final accuracy as these methods are not true *streaming learning* method.

Table 8 categorizes the baselines according to the underlying assumptions that they impose. For baselines which finetunes the network before inference and violates the constraint of *streaming learning*, such as *single pass learning* constraint, have been marked in red in the corresponding column.

## D. Ablation Study Additional Results

In this section, we provide additional results for ablation studies, which we could not provide in the main paper due to space constraints.

- **ImageNet100**. In Table 9, we compare the final  $\Omega_{\text{all}}$  accuracy of CIOSL for (i) i.i.d, and (ii) class-i.i.d ordering on Imagenet100 dataset while using different memory replacement policy and past sample selection strategies.
- **CIFAR10/100**. Table 10 compares the final  $\Omega_{\text{all}}$  accuracy of the proposed model (CIOSL) for (i) i.i.d and (ii) class-i.i.d ordering on CIFAR10 and CIFAR100 respectively while using different values for the knowledge-distillation hyper-parameter  $\lambda_2$ , and different memory replacement policies and various sample selection strategies.

- **iCubWorld 1.0**. Table 11 and Table 12 compares the final  $\Omega_{\text{all}}$  accuracy of CIOSL for (i) i.i.d, (ii) class-i.i.d, (iii) instance, and (iv) class-instance ordering on iCubWorld 1.0 dataset while using different knowledge-distillation hyper-parameter  $\lambda_2$  and different sampling strategies. For memory replacement policy, Table 11 uses ‘*loss-aware weighted class balancing replacement (LAWCBR)*’ strategy, whereas Table 12 uses ‘*loss-aware weighted random replacement with a reservoir (LAWRRR)*’ strategy.

## E. ImageNet-100

In this paper, we used a subset of ImageNet-1000 (ILSVRC-2012) [36] that contains randomly chosen 100 classes. To ease a relevant study, we release the list of these 100 classes that we used to evaluate the streaming learner’s performance in our experiments, as mentioned in Table 14.

## F. Additional Implementation Details

In this section, we provide some additional implementation details, which we could not provide in the main paper due to space constraints.

We use Mobilenet-V2 [38] pre-trained on ImageNet [36] available in PyTorch [32] TorchVision package as the base architecture for the feature extractor  $G(\cdot)$ . We use the convolutional base of Mobilenet-V2 [38] as the feature extractor  $G(\cdot)$  to obtain embeddings from the raw pixels; we keep it frozen throughout the streaming learning. We use *uniform sampling* and knowledge-distillation hyper-parameter  $\lambda_2 = 0.2$  for *online learning* and *batch learning* experiments (in Table 5). We provide the parameter settings for the proposed method (CIOSL) and the offline models in Table 13.

## G. Evaluation Over Different Data Orderings Additional Details

The proposed approach (CIOSL) is robust to various *streaming learning scenarios* that can induce catastrophic forgetting [12]. We evaluate the model’s streaming learning ability with the four challenging data ordering [14, 15] schemes: (i) ‘*streaming iid*’, (ii) ‘*streaming class iid*’, (iii) ‘*streaming instance*’, and (iv) ‘*streaming class instance*’. We described this four data ordering schemes in more detail in Section 5.2 in the main paper.

**Note:** Only iCubWorld 1.0 [9] dataset contains the temporal ordering, therefore, ‘*streaming instance*’ ‘*streaming class instance*’ setting evaluated only on the iCubWorld 1.0 dataset.

In the below, we describe the following: (i) how the base initialization is performed, and (ii) how the network is trained in *streaming setting* according to various data ordering schemes on different datasets.

Method	Learning Type	Fine-tunes	Violates Constraints Of Streaming Learning	Regularize	Memory
EWC	Batch	✗	✗	✓	✗
MAS	Batch	✗	✗	✓	✗
VCL	Batch	✗	✗	✓	✗
VCL w/ C/	Batch	✓	✓	✓	✓
Coreset	Online	✓	✓	✗	✓
GDumb	Online	✓	✓	✗	✓
TinyER	Online	✗	✗	✗	✓
A-GEM	Online	✗	✗	✓	✓
ExStream	Streaming	✗	✗	✗	✓
REMIND	Streaming	✗	✗	✗	✓
<b>Ours</b>	Streaming	✗	✗	✓	✓

Table 8. Categorization of the baseline approaches depending on the underlying simplifying assumptions they impose.

Memory Replacement	Sample Selection	Imagenet100	
		iid	Class-iid
LAWCBR	Uni	0.9582 ± 0.0037	0.9014 ± 0.0073
	UAPN	0.9327 ± 0.0052	0.9135 ± 0.0081
	LAPN	0.9253 ± 0.0115	0.9122 ± 0.0091
LAWRRR	Uni	<b>0.9640 ± 0.0060</b>	0.8643 ± 0.0127
	UAPN	0.9578 ± 0.0035	<b>0.9171 ± 0.0073</b>
	LAPN	0.9575 ± 0.0047	0.9112 ± 0.0075

Table 9.  $\Omega_{\text{all}}$  Results as a function of different memory replacement policies and sample selection strategies for (i) i.i.d, and (ii) class-i.i.d ordering on ImageNet100.

## G.1. CIFAR10

CIFAR10 [24] is a standard image classification dataset. It contains 10 classes with each consists of 5000 training images and 1000 testing images. Since, it does not contain any temporally ordered image sequence, we use CIFAR10 to evaluate the *streaming learner's* ability in *streaming i.i.d* and *streaming class-i.i.d* orderings.

- **streaming i.i.d:** For the base initialization, we randomly select 2% samples from the dataset and train the model in offline manner. Then we randomly shuffle the remaining samples and train the model incrementally with these samples by feeding one at a time in a streaming manner.
- **streaming class-i.i.d:** In base initialization, the model is trained in a typical offline mode with the samples from the first two classes. Then, in each incremental step, we select the samples from the next two classes, which are not included earlier. These samples are randomly shuffled and fed into the model in a streaming manner.

## G.2. CIFAR100

CIFAR100 [24] is another standard image classification dataset. It contains 100 classes with each consists of 500 training images and 100 testing images. We use CIFAR100 to evaluate the model's ability in *streaming i.i.d* and *streaming class-i.i.d* orderings.

- **streaming i.i.d:** In this setting, we follow the similar approach as mentioned for the CIFAR10 dataset, with the only exception is that the base initialization is performed with 10% randomly chosen samples, and the remaining samples are used for streaming learning.
- **streaming class-i.i.d:** This approach also follows the similar approach as mentioned for the CIFAR10 dataset. However, in each incremental step, including the base initialization, we use samples from 10 classes. For the base initialization, we select samples from the first ten classes, and in each incremental step, we select samples from the succeeding ten classes which are not observed earlier.

## G.3. ImageNet100

ImageNet100 is a subset of ImageNet-1000 (ILSVRC-2012) [36] that contains randomly chosen 100 classes, with each classes containing 700 – 1300 training samples and 50 validation samples. Since, for test samples, we do not have the ground truth labels, we use the validation data for testing the model's accuracy. We provide more details on ImageNet100 in Section E.

We use ImageNet100 dataset to evaluate the model's ability in *streaming i.i.d* and *streaming class-i.i.d* orderings.

- **streaming i.i.d:** In this case, we follow the similar approach as mentioned for CIFAR100 *streaming i.i.d* ordering.

$\lambda_2$	Memory Replacement	Sample Selection	iid		class-iid	
			CIFAR10	CIFAR100	CIFAR10	CIFAR100
0.2	LAWCBR	Uni	0.9542 $\pm$ 0.0053	0.8135 $\pm$ 0.0054	0.8942 $\pm$ 0.0062	0.7343 $\pm$ 0.0131
		UAPN	0.9084 $\pm$ 0.0121	0.4760 $\pm$ 0.0136	0.8957 $\pm$ 0.0125	0.6448 $\pm$ 0.0257
		LAPN	0.8462 $\pm$ 0.0414	0.3834 $\pm$ 0.0335	0.8797 $\pm$ 0.0149	0.5332 $\pm$ 0.0310
	LAWRRR	Uni	<b>0.9584 <math>\pm</math> 0.0035</b>	0.8617 $\pm$ 0.0091	0.8792 $\pm$ 0.0104	0.7221 $\pm$ 0.0149
		UAPN	0.9567 $\pm$ 0.0031	0.8366 $\pm$ 0.0107	0.8978 $\pm$ 0.0107	0.7589 $\pm$ 0.0185
		LAPN	0.9530 $\pm$ 0.0037	0.8273 $\pm$ 0.0141	0.8986 $\pm$ 0.0127	0.7478 $\pm$ 0.0191
0.3	LAWCBR	Uni	0.9529 $\pm$ 0.0062	0.8134 $\pm$ 0.0077	0.8970 $\pm$ 0.0088	0.7369 $\pm$ 0.0106
		UAPN	0.9145 $\pm$ 0.0071	0.5096 $\pm$ 0.0088	0.8944 $\pm$ 0.0093	0.6836 $\pm$ 0.0231
		LAPN	0.9046 $\pm$ 0.0152	0.4376 $\pm$ 0.0220	0.8798 $\pm$ 0.0230	0.6275 $\pm$ 0.0291
	LAWRRR	Uni	0.9579 $\pm$ 0.0040	<b>0.8679 <math>\pm</math> 0.0057</b>	0.8838 $\pm$ 0.0088	0.7307 $\pm$ 0.0122
		UAPN	0.9567 $\pm$ 0.0031	0.8542 $\pm$ 0.0066	0.8991 $\pm$ 0.0089	<b>0.7724 <math>\pm</math> 0.0188</b>
		LAPN	0.9538 $\pm$ 0.0044	0.8453 $\pm$ 0.0120	<b>0.9024 <math>\pm</math> 0.0116</b>	0.7573 $\pm$ 0.0193

Table 10.  $\Omega_{\text{all}}$  Results as a function of knowledge-distillation hyper-parameter  $\lambda_2$  and different memory replacement policies and sample selection strategies for (i) i.i.d ordering, and (ii) class-i.i.d ordering on CIFAR10 and CIFAR100 datasets.

$\lambda_2$	Sample Selection	iCubWorld 1.0			
		iid	Class-iid	Instance	Class-instance
0.0	Uni	0.9431 $\pm$ 0.0418	0.9105 $\pm$ 0.0333	0.8414 $\pm$ 0.0541	0.8259 $\pm$ 0.0316
	UAPN	0.8775 $\pm$ 0.0753	0.8863 $\pm$ 0.0529	0.6777 $\pm$ 0.0764	0.7711 $\pm$ 0.0574
	LAPN	0.8975 $\pm$ 0.0697	0.8675 $\pm$ 0.0498	0.7576 $\pm$ 0.0739	0.7524 $\pm$ 0.0655
0.1	Uni	<b>0.9885 <math>\pm</math> 0.0245</b>	0.9163 $\pm$ 0.0237	0.9257 $\pm$ 0.0299	0.8369 $\pm$ 0.0329
	UAPN	0.9781 $\pm$ 0.0318	0.9167 $\pm$ 0.0263	0.9124 $\pm$ 0.0525	0.8627 $\pm$ 0.0285
	LAPN	0.9779 $\pm$ 0.0206	0.9224 $\pm$ 0.0332	0.8988 $\pm$ 0.0544	0.8543 $\pm$ 0.0288
0.2	Uni	0.9841 $\pm$ 0.0178	0.9154 $\pm$ 0.0217	0.9219 $\pm$ 0.0333	0.8454 $\pm$ 0.0283
	UAPN	0.9868 $\pm$ 0.0181	0.9293 $\pm$ 0.0306	0.9152 $\pm$ 0.0229	<b>0.8712 <math>\pm</math> 0.0266</b>
	LAPN	0.9645 $\pm$ 0.0189	0.9310 $\pm$ 0.0227	0.9030 $\pm$ 0.0503	0.8516 $\pm$ 0.0400
0.3	Uni	0.9777 $\pm$ 0.0264	0.9257 $\pm$ 0.0288	0.8975 $\pm$ 0.0454	0.8506 $\pm$ 0.0310
	UAPN	0.9868 $\pm$ 0.0125	0.9309 $\pm$ 0.0355	<b>0.9346 <math>\pm</math> 0.0395</b>	0.8500 $\pm$ 0.0363
	LAPN	0.9745 $\pm$ 0.0174	<b>0.9352 <math>\pm</math> 0.0266</b>	0.9172 $\pm$ 0.0373	0.8536 $\pm$ 0.0343
0.4	Uni	0.9782 $\pm$ 0.0200	0.9278 $\pm$ 0.0295	0.9112 $\pm$ 0.0327	0.8377 $\pm$ 0.0292
	UAPN	0.9815 $\pm$ 0.0178	0.9160 $\pm$ 0.0464	0.8988 $\pm$ 0.0419	0.8509 $\pm$ 0.0350
	LAPN	0.9718 $\pm$ 0.0271	0.9325 $\pm$ 0.0401	0.9243 $\pm$ 0.0512	0.8499 $\pm$ 0.0650
0.5	Uni	0.9742 $\pm$ 0.0183	0.8858 $\pm$ 0.1505	0.9341 $\pm$ 0.0350	0.7787 $\pm$ 0.2008
	UAPN	0.9692 $\pm$ 0.0197	0.8587 $\pm$ 0.2278	0.9082 $\pm$ 0.0758	0.7914 $\pm$ 0.2033
	LAPN	0.9725 $\pm$ 0.0184	0.9006 $\pm$ 0.0635	0.9129 $\pm$ 0.0467	0.8357 $\pm$ 0.0334

Table 11.  $\Omega_{\text{all}}$  Results as a function of knowledge-distillation hyper-parameter  $\lambda_2$ , and ‘loss-aware weighted class balancing replacement’ (LAWCBR) and different sampling strategies for (i) i.i.d, (ii) class-i.i.d, (iii) instance, and (iv) class-instance ordering on iCubWorld 1.0 dataset.

- **streaming class-i.i.d:** We follow the similar approach as has been mentioned for CIFAR100 *streaming class-i.i.d* ordering.

#### G.4. iCubWorld 1.0

iCubWorld 1.0 [9] is an object recognition dataset containing the sequence of video frames, with each frame con-

taining only a single object. It is a more challenging and realistic dataset w.r.t the other standard datasets such as CIFAR10, CIFAR100, and ImageNet100. Technically, it is an ideal dataset to evaluate a model’s performance in *streaming learning* scenarios that are known to induce catastrophic forgetting [12], as it requires learning from temporally ordered image sequences, which are naturally *non-i.i.d* images.

$\lambda_2$	Sample Selection	iCubWorld 1.0			
		iid	Class-iid	Instance	Class-instance
0.0	Uni	0.9298 $\pm$ 0.0329	0.9063 $\pm$ 0.0396	0.8837 $\pm$ 0.0544	0.9168 $\pm$ 0.0312
	UAPN	0.9184 $\pm$ 0.0379	0.8818 $\pm$ 0.0396	0.7507 $\pm$ 0.0732	0.8384 $\pm$ 0.0675
	LAPN	0.9285 $\pm$ 0.0357	0.8912 $\pm$ 0.0430	0.7735 $\pm$ 0.0458	0.8657 $\pm$ 0.0521
0.1	Uni	<b>0.9830 <math>\pm</math> 0.0207</b>	0.9240 $\pm$ 0.0276	0.9292 $\pm$ 0.0344	0.9162 $\pm$ 0.0255
	UAPN	0.9644 $\pm$ 0.0260	0.9368 $\pm$ 0.0228	0.9439 $\pm$ 0.0362	0.9411 $\pm$ 0.0224
	LAPN	0.9541 $\pm$ 0.0280	0.9402 $\pm$ 0.0368	0.9241 $\pm$ 0.0401	0.9345 $\pm$ 0.0235
0.2	Uni	0.9600 $\pm$ 0.0312	0.9351 $\pm$ 0.0315	0.9155 $\pm$ 0.0299	0.9229 $\pm$ 0.0284
	UAPN	0.9640 $\pm$ 0.0236	0.9415 $\pm$ 0.0307	0.9254 $\pm$ 0.0331	0.9468 $\pm$ 0.0273
	LAPN	0.9684 $\pm$ 0.0160	0.9382 $\pm$ 0.0361	0.9368 $\pm$ 0.0376	0.9454 $\pm$ 0.0263
0.3	Uni	0.9716 $\pm$ 0.0141	0.9118 $\pm$ 0.0344	0.9269 $\pm$ 0.0383	0.9346 $\pm$ 0.0191
	UAPN	0.9454 $\pm$ 0.0239	0.9480 $\pm$ 0.0215	<b>0.9580 <math>\pm</math> 0.0298</b>	<b>0.9585 <math>\pm</math> 0.0223</b>
	LAPN	0.9667 $\pm$ 0.0174	<b>0.9538 <math>\pm</math> 0.0303</b>	0.9558 $\pm$ 0.0304	0.9497 $\pm$ 0.0239
0.4	Uni	0.9611 $\pm$ 0.0153	0.9243 $\pm$ 0.0524	0.9350 $\pm$ 0.0319	0.9222 $\pm$ 0.0403
	UAPN	0.9647 $\pm$ 0.0257	0.9387 $\pm$ 0.0315	0.9476 $\pm$ 0.0264	0.9005 $\pm$ 0.1257
	LAPN	0.9615 $\pm$ 0.0194	0.9323 $\pm$ 0.0421	0.9257 $\pm$ 0.0212	0.9509 $\pm$ 0.0323
0.5	Uni	0.9615 $\pm$ 0.0301	0.9391 $\pm$ 0.0268	0.9001 $\pm$ 0.0555	0.9145 $\pm$ 0.0649
	UAPN	0.9526 $\pm$ 0.0179	0.9390 $\pm$ 0.0267	0.9275 $\pm$ 0.0322	0.8766 $\pm$ 0.2320
	LAPN	0.9495 $\pm$ 0.0215	0.9085 $\pm$ 0.1230	0.9369 $\pm$ 0.0187	0.9533 $\pm$ 0.0248

Table 12.  $\Omega_{\text{all}}$  Results as a function of knowledge-distillation hyper-parameter  $\lambda_2$ , and ‘loss-aware weighted random replacement with a reservoir’ (LAWRRR) and different sampling strategies for (i) i.i.d, (ii) class-i.i.d, (iii) instance, and (iv) class-instance ordering on iCubWorld 1.0 dataset.

Parameters	Datasets			
	CIFAR10	CIFAR100	ImageNet100	iCubWorld 1.0
Optimizer	SGD	SGD	SGD	SGD
Learning Rate	0.01	0.01	0.01	0.01
Momentum	0.9	0.9	0.9	0.9
Weight Decay	1e-05	1e-05	1e-05	1e-05
Hidden Layer	[256, 256]	[256, 256]	[256, 256]	[256, 256]
Activation	ReLU	ReLU	ReLU	ReLU
Offline Batch Size	128	128	256	16
Offline Epoch	50	50	100	30
Buffer Capacity	1000	1000	1000	180
Train-Set Size	50000	50000	127778	6002

Table 13. Training parameters used for CIOSL and Offline model.

It contains 10 classes, each with 3 different object instances with 200 – 201 images each. Overall, each class contains 600 – 602 samples for training and 200 – 201 samples for testing. Figure 6 shows example images of the 30 object instances in iCubWorld 1.0, where each row denotes one of the 10 categories.

We use iCubWorld 1.0 to evaluate the performance of the streaming learner’s in all the four data ordering schemes, i.e., (i) *streaming i.i.d*, (ii) *streaming class-i.i.d*, (iii) *streaming instance*, and (iv) *streaming class-instance*.

- **streaming i.i.d:** In this setting, we follow the similar

approach as mentioned for the CIFAR10 dataset, with the only exception, that is, 10% randomly selected samples are used for the base initialization, and the rest are used for streaming learning.

- **streaming class-i.i.d:** In this case, we follow the same strategy as mentioned for CIFAR10 *streaming class-i.i.d* ordering.
- **streaming class-instance:** In base initialization, the model is trained in a typical offline mode with the samples from the first two classes. In each incremental step,

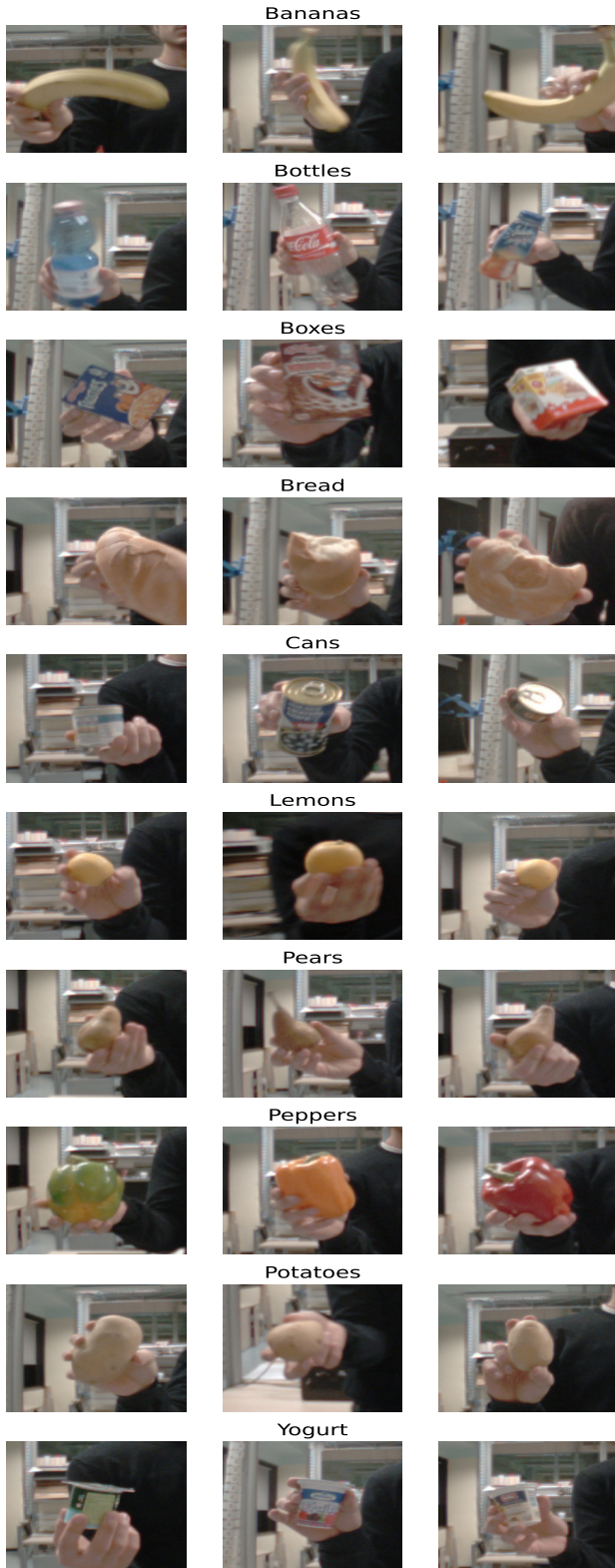


Figure 6. The iCubWorld 1.0 [9] dataset. 10 categories: Bananas, Bottles, Boxes, Bread, Cans, Lemons, Pears, Peppers, Potatoes, Yogurt. Each category contains 3 different instances.

List Of ImageNet-100 Classes

n01632777	n01667114	n01744401	n01753488
n01768244	n01770081	n01798484	n01829413
n01843065	n01871265	n01872401	n01981276
n02006656	n02012849	n02025239	n02085620
n02086079	n02089867	n02091831	n02094258
n02096294	n02100236	n02100877	n02102040
n02105251	n02106550	n02110627	n02120079
n02130308	n02168699	n02169497	n02177972
n02264363	n02417914	n02422699	n02437616
n02483708	n02488291	n02489166	n02494079
n02504013	n02667093	n02687172	n02788148
n02791124	n02794156	n02814860	n02859443
n02895154	n02910353	n03000247	n03208938
n03223299	n03271574	n03291819	n03347037
n03445777	n03529860	n03530642	n03602883
n03627232	n03649909	n03666591	n03761084
n03770439	n03773504	n03788195	n03825788
n03866082	n03877845	n03908618	n03916031
n03929855	n03954731	n04009552	n04019541
n04141327	n04147183	n04235860	n04285008
n04286575	n04328186	n04347754	n04355338
n04423845	n04442312	n04456115	n04485082
n04486054	n04505470	n04525038	n07248320
n07716906	n07730033	n07768694	n07836838
n07860988	n07871810	n11939491	n12267677

Table 14. The list of classes from ImageNet-100, which are randomly chosen from the original ImageNet-1000 (ILSVRC-2012) [36].

the network is trained in a streaming manner with the samples from the succeeding two classes which were not observed earlier. However, in this case, (i) samples within a class are temporally ordered based on different object instances, and (ii) all samples from one class are fed into the network before feeding any samples from the other class.

- **streaming instance:** For the base initialization, 10% randomly chosen samples are used, and the remaining samples are used to train the model incrementally with one sample at a time. In streaming setting, the samples are temporally ordered based on different object instances. Specifically, we organize the data stream by putting temporally ordered 50 frames of an object instance, then we put temporally ordered 50 frames of the second object instance, and so on. In this way, after putting 50 temporally ordered frames from each object instance, we put the next 50 temporally ordered frames of the first object instance and follow the earlier approach until all the frames of each instance have been exhausted.

## H. Derivation of Joint Posterior

$$\begin{aligned}
\mathcal{L}_t^1(\boldsymbol{\theta}) &= \arg \min_{q \in \mathcal{Q}} \text{KL} \left[ q_t(\boldsymbol{\theta}) \parallel \frac{1}{Z_t} q_{t-1}(\boldsymbol{\theta}) p(\mathcal{D}_t | \boldsymbol{\theta}) p(\mathcal{D}_{\mathcal{M},t} | \boldsymbol{\theta}) \right] \\
&\simeq \arg \min_{q \in \mathcal{Q}} \text{KL} [q_t(\boldsymbol{\theta}) | | q_{t-1}(\boldsymbol{\theta}) p(\mathcal{D}_t | \boldsymbol{\theta}) p(\mathcal{D}_{\mathcal{M},t} | \boldsymbol{\theta})] \\
&= \int q_t(\boldsymbol{\theta}) \log \frac{q_t(\boldsymbol{\theta})}{q_{t-1}(\boldsymbol{\theta}) p(\mathcal{D}_t | \boldsymbol{\theta}) p(\mathcal{D}_{\mathcal{M},t} | \boldsymbol{\theta})} d\boldsymbol{\theta} \\
&= - \int q_t(\boldsymbol{\theta}) \log \frac{q_{t-1}(\boldsymbol{\theta}) p(\mathcal{D}_t | \boldsymbol{\theta}) p(\mathcal{D}_{\mathcal{M},t} | \boldsymbol{\theta})}{q_t(\boldsymbol{\theta})} d\boldsymbol{\theta} \\
&= \arg \max \int q_t(\boldsymbol{\theta}) \log \frac{q_{t-1}(\boldsymbol{\theta}) p(\mathcal{D}_t | \boldsymbol{\theta}) p(\mathcal{D}_{\mathcal{M},t} | \boldsymbol{\theta})}{q_t(\boldsymbol{\theta})} d\boldsymbol{\theta} \\
&= \int q_t(\boldsymbol{\theta}) \log p(\mathcal{D}_t | \boldsymbol{\theta}) p(\mathcal{D}_{\mathcal{M},t} | \boldsymbol{\theta}) d\boldsymbol{\theta} \\
&\quad + \int q_t(\boldsymbol{\theta}) \log \frac{q_{t-1}(\boldsymbol{\theta})}{q_t(\boldsymbol{\theta})} d\boldsymbol{\theta} \\
&= \int q_t(\boldsymbol{\theta}) \log p(\mathcal{D}_t | \boldsymbol{\theta}) d\boldsymbol{\theta} + \int q_t(\boldsymbol{\theta}) \log p(\mathcal{D}_{\mathcal{M},t} | \boldsymbol{\theta}) d\boldsymbol{\theta} \\
&\quad - \int q_t(\boldsymbol{\theta}) \log \frac{q_t(\boldsymbol{\theta})}{q_{t-1}(\boldsymbol{\theta})} d\boldsymbol{\theta} \\
&= \mathbb{E}_{\boldsymbol{\theta} \sim q_t(\boldsymbol{\theta})} [\log p(\mathcal{D}_t | \boldsymbol{\theta})] + \mathbb{E}_{\boldsymbol{\theta} \sim q_t(\boldsymbol{\theta})} [\log p(\mathcal{D}_{\mathcal{M},t} | \boldsymbol{\theta})] \\
&\quad - \text{KL} [q_t(\boldsymbol{\theta}) | | q_{t-1}(\boldsymbol{\theta})] \\
&= \mathbb{E}_{\boldsymbol{\theta} \sim q_t(\boldsymbol{\theta})} [\log p(\mathcal{D}_t | \boldsymbol{\theta})] + \mathbb{E}_{\boldsymbol{\theta} \sim q_t(\boldsymbol{\theta})} [\log p(\mathcal{D}_{\mathcal{M},t} | \boldsymbol{\theta})] \\
&\quad - \lambda_1 \text{KL} [q_t(\boldsymbol{\theta}) | | q_{t-1}(\boldsymbol{\theta})] \\
&= \arg \max \mathbb{E}_{\boldsymbol{\theta} \sim q_t(\boldsymbol{\theta})} [\log p(y_t | \boldsymbol{\theta}, G(\boldsymbol{x}_t))] \\
&\quad + \sum_{n=1}^{N'_1} \mathbb{E}_{\boldsymbol{\theta} \sim q_t(\boldsymbol{\theta})} \left[ \log p(y_{\mathcal{M},t}^{(n)} | \boldsymbol{\theta}, \boldsymbol{z}_{\mathcal{M},t}^{(n)}) \right] \\
&\quad - \lambda_1 \cdot \text{KL} (q_t(\boldsymbol{\theta}) | | q_{t-1}(\boldsymbol{\theta}))
\end{aligned}$$

where  $\mathcal{D}_t = \{\boldsymbol{d}_t\} = \{(\boldsymbol{x}_t, y_t)\}$ ,  $\mathcal{D}_{\mathcal{M},t} = \{\boldsymbol{d}_{\mathcal{M},t}^{(n)}\}_{n=1}^{N'_1} = \{(\boldsymbol{z}_{\mathcal{M},t}^{(n)}, y_{\mathcal{M},t}^{(n)})\}_{n=1}^{N'_1}$ ,  $|\mathcal{D}_{\mathcal{M},t}| = N'_1 \ll |\mathcal{M}|$ ,  $\mathcal{D}_{\mathcal{M},t} \subset \mathcal{M}$ , and  $\lambda_1$  is a hyper-parameter.